

---

# Radiotargeted Gene Therapy

Donald J. Buchsbaum, PhD<sup>1</sup>; Tandra R. Chaudhuri, PhD<sup>2</sup>; and Kurt R. Zinn, DVM, PhD<sup>3</sup>

<sup>1</sup>Department of Radiation Oncology, University of Alabama at Birmingham, Birmingham, Alabama; <sup>2</sup>Department of Radiology, University of Alabama at Birmingham, Birmingham, Alabama; and <sup>3</sup>Department of Medicine, University of Alabama at Birmingham, Birmingham, Alabama

---

The radiotargeted gene therapy approach to localizing radionuclides at tumor sites involves inducing tumor cells to synthesize a membrane-expressed receptor with a high affinity for injected radiolabeled ligands. A second strategy involves transduction of the sodium iodide symporter (NIS) and free radionuclide therapy. Using the first strategy, induction of high levels of human somatostatin receptor subtype 2 expression and selective tumor uptake, imaging, or growth inhibition with radiolabeled somatostatin analogs has been achieved in human tumor xenograft models. Therapy studies have been performed on several tumor xenograft models with various radionuclides using the NIS radiotargeted gene therapy approach. The use of gene transfer technology to induce expression of high-affinity membrane receptors or transporters can enhance the specificity and extent of radioligand or radionuclide localization in tumors, and the use of radionuclides with appropriate emissions can deliver radiation-absorbed cytotoxic doses across several cell diameters to compensate for limited transduction efficiency. Clinical studies are needed to determine the most promising of these new therapeutic approaches.

**Key Words:** human somatostatin receptor subtype 2; sodium iodide symporter; gene therapy; radiopharmaceuticals; radiolabeled peptides

**J Nucl Med 2005; 46:179S–186S**

---

**R**adiolabeled somatostatin analogs (e.g., <sup>111</sup>In-pentetreotide [OctreoScan; Mallinckrodt Inc.] or <sup>99m</sup>Tc-depreotide [Neotect; Diatide Inc.]) have been used to target human somatostatin receptor subtype 2 (hSSTR2)-positive tumor cells for imaging of patients (1,2). The peptides have been labeled with various radionuclides for therapeutic applications, which have been performed on preclinical animal models (3–5) and on cancer patients (6,7). Despite the success of these investigations, improved targeting strategies are needed to produce an even greater effect in the treatment of cancer. One approach is to use gene transfer methods to upregulate tumor-associated receptor expression, followed by systemic administration of radiolabeled peptide. We have developed replication-defective adenovi-

ral (Ad) recombinant vectors that transfer the hSSTR2-encoding gene to tumors, enhancing uptake of radiolabeled somatostatin peptide analogs to tumor cells. The use of these vectors to produce preferential tumor localization of radiolabeled somatostatin analogs in animal xenograft models has been described (8–11). A potential advantage of genetic transduction of hSSTR2 is that the level of expression may be greater than what are the generally otherwise low tumor concentrations of such receptors.

A second approach to radiotargeted gene therapy is the transduction of tumors with transporters such as the sodium iodide symporter (NIS) gene, which is responsible for the active uptake and concentration of iodide, pertechnetate, perrhenate, and astatide (12–14). Both approaches for radiotargeted gene therapy may be enhanced by codelivery of a second therapeutic gene such as herpes virus thymidine kinase (TK) or cytosine deaminase (CD) to accomplish molecular prodrug therapy (11,15). That therapeutic approach involves insertion and expression of an enzyme in a target cell that converts a nontoxic prodrug to a toxic drug. Two of the most widely studied systems are TK and CD. Transduction of tumor cells with the TK gene phosphorylates nucleoside prodrugs such as ganciclovir (GCV), resulting in inhibition of DNA synthesis and cell death. CD is a nonmammalian enzyme that catalyzes the formation of uracil by the deamination of cytosine. When 5-fluorocytosine (5-FC) is the substrate, CD will produce 5-fluorouracil, a cancer chemotherapeutic and radiosensitizing agent. The CD gene has been used successfully in gene therapy studies in animal tumor models. Results reported by our group and other investigators involving combination of radiation therapy with molecular prodrug therapy have shown that CD-based prodrug therapy sensitizes tumor cells to external-beam radiation both *in vitro* and *in vivo* (16). Studies involving combination of radiolabeled peptide therapy with molecular prodrug therapy are described in this article.

Linking tumor transduction of the hSSTR2 or the NIS to induced binding of radiolabeled ligands or radionuclides might enhance the therapeutic effect, since cells near bound ligand or internalized radionuclide may be killed from exposure to the local radiation field. When used with radionuclide therapy, uniform systemic incorporation of the genetic construct into tumor cells is not necessary, because of this crossfire effect. There are 2 potential advantages to the

---

Received May 7, 2004; revision accepted Aug. 13, 2004.  
For correspondence or reprints contact: Donald J. Buchsbaum, PhD, Department of Radiation Oncology, University of Alabama at Birmingham, 1530 3rd Ave. S., WTI 674, Birmingham, AL 35294-6832.  
E-mail: djb@uab.edu

genetic transduction approach: Constitutive expression of a tumor-associated receptor or transporter is not required, and tumor cells are altered to express a new target receptor or transporter at levels that increase tumor targeting of radio-labeled ligands or free radionuclides and increase therapeutic efficacy.

The target of many therapy studies with radiolabeled peptides has been hSSTR2, which is expressed on several human tumors including neuroendocrine, ovary, kidney, breast, prostate, lung, and meningioma tumors (17). The somatostatin receptor group includes gene products encoded by 5 separate somatostatin receptor genes. Somatostatin receptor subtype 2 is the most prominent somatostatin receptor on human tumors. The receptors are expressed at varying levels in the brain, gastrointestinal tract, pancreas, kidney, and spleen. All 5 receptors show high-affinity binding to natural somatostatin peptide (either somatostatin-14 or somatostatin-28). Octreotide, P829, and P2045 are synthetic somatostatin analogs that preferentially bind with high affinity to somatostatin receptor subtypes 2, 3, and 5 of human, mouse, or rat origin (18–20). Somatostatin and its analogs effectively inhibit the proliferation of various types of cancer cells as a result of binding to hSSTR2 (21).

Octreotide is an 8-amino-acid peptide that has a high affinity for hSSTR2 and is stable toward *in vivo* degradation relative to the endogenous 14-amino-acid somatostatin-14 peptide. Octreotide and other somatostatin analogs have been conjugated with bifunctional chelating agents, for complexing radiometals, and their amino acid sequence changed to increase their hSSTR2 binding affinity and optimize their normal organ clearance. Somatostatin analogs have been labeled with several radionuclides, including <sup>111</sup>In, <sup>90</sup>Y, <sup>64</sup>Cu, <sup>177</sup>Lu, and <sup>188</sup>Re, for therapeutic applications in preclinical models (3–5,22) or clinical trials (23–25). <sup>90</sup>Y-1,4,7,10-tetraazacyclododecane-*N,N',N'',N'''*-tetraacetic acid (DOTA)-*D*-Phe<sup>1</sup>-Tyr<sup>3</sup>-octreotide (SMT 487) was administered to patients with malignant tumors (carcinoids, breast cancer, medullary thyroid cancer, meningioma) in a phase I trial (23). Complete and partial responses were obtained in 25% of patients, and 55% showed stable disease lasting at least 3 mo. Thus, several radiolabeled somatostatin analogs have shown potential as radiotherapeutic agents in animal tumor models and in humans.

## STUDIES COMBINING RADIOTHERAPY AND MOLECULAR PRODRUG THERAPY

### Study Descriptions

A replication-incompetent Ad vector encoding the gene for hSSTR2 (subtype a) under control of the cytomegalovirus promoter (AdCMVhSSTR2) was produced (8). *In vitro* binding of <sup>125</sup>I-somatostatin, <sup>99m</sup>Tc-P829 (<sup>99m</sup>Tc-depreotide), and <sup>111</sup>In-diethylenetriaminepentaacetic acid (DTPA)-*D*-Phe<sup>1</sup>-octreotide (<sup>111</sup>In-pentetreotide) to cells or cell membrane preparations of human ovarian and non-small cell lung cancer cells infected with AdCMVhSSTR2 was shown by imaging of cells in plates (26) or counting of cell membrane preparations (8). To evaluate the ability to induce

receptor expression in an animal model, AdCMVhSSTR2 was injected intraperitoneally into athymic nude mice bearing SK-OV-3.ip1 human ovarian tumors in the peritoneum.  $\gamma$ -Camera imaging was used to detect hSSTR2 expression in subcutaneous A-427 non-small cell lung tumors injected with AdCMVhSSTR2 using <sup>188</sup>Re-P829 somatostatin analog (9).

<sup>99m</sup>Tc-P2045 binds with high affinity to hSSTR2 and has favorable *in vivo* biodistribution (19). <sup>99m</sup>Tc-P2045 tumor uptake was evaluated in mice bearing SK-OV-3.ip1 tumors in the peritoneum injected intraperitoneally with AdCMVhSSTR2 ( $1 \times 10^9$  plaque-forming units [pfu]). In another study, <sup>99m</sup>Tc-P2045 was injected intravenously 2 or 4 d after AdCMVhSSTR2 intratumoral injection in mice bearing subcutaneous A-427 tumors, and the animals were imaged using a  $\gamma$ -camera 3.5–4.5 h later.

Tumor localization of <sup>64</sup>Cu-1,4,8,11-tetraazacyclotetradecane-*N,N',N'',N'''*-tetraacetic acid (TETA)-octreotide was studied in mice bearing intraperitoneal SK-OV-3.ip1 human ovarian tumors induced to express hSSTR2 with AdCMVhSSTR2. <sup>64</sup>Cu is a potentially therapeutic radionuclide that can be imaged by PET. In a therapy study, a single administration of 51.8 or 74 MBq of <sup>64</sup>Cu-TETA-octreotide 2 d after AdCMVhSSTR2 injection was used in mice bearing intraperitoneal SK-OV-3.ip1 tumors. Also, 51.8 MBq of <sup>64</sup>Cu-TETA-octreotide was administered 2 d after AdCMVhSSTR2 injection, followed by a second dose of AdCMVhSSTR2 11 d later and administration of 25.9 MBq of <sup>64</sup>Cu-TETA-octreotide 2 d afterward.

Another somatostatin analog that has been used for therapy is <sup>90</sup>Y-SMT 487 (4,23). Nude mice bearing subcutaneous A-427 tumors were administered  $1 \times 10^9$  pfu of AdCMVhSSTR2 intratumorally (day 0). Mice received an intravenous injection of either 14.8 or 18.5 MBq of <sup>90</sup>Y-SMT 487 on days 2 and 4. The mice received an additional intratumoral injection of AdCMVhSSTR2 on day 7, followed by 2 more 14.8- or 18.5-MBq doses of <sup>90</sup>Y-SMT 487 on days 9 and 11. Control tumor-bearing mice either did not receive treatment or received four 18.5-MBq doses of <sup>90</sup>Y-SMT 487 on days 2, 4, 9, and 11 without AdCMVhSSTR2 injections (27).

Ad vectors were produced expressing hSSTR2 with a second therapeutic gene (TK or CD). This offers the potential for combination therapy using radiolabeled somatostatin analogs and prodrugs such as GCV or 5-FC. Localization and imaging studies were performed using a bicistronic nonreplicative Ad vector encoding hSSTR2 and TK in a non-small cell lung cancer xenograft model (11). The A-427 tumors were injected intratumorally with the bicistronic vector (AdCMVhSSTR2TK), and the animals were imaged for hSSTR2 expression with <sup>99m</sup>Tc-P2045 and TK with <sup>131</sup>I-2'-fluoro-2'-deoxy-1- $\beta$ -D-arabinofuranosyl-5-iodouracil (FIAU).

Bicistronic Ad vectors encoding for hSSTR2 and the TK enzyme were constructed and evaluated (11). The rationale for the construction of these vectors is 2-fold. First, hSSTR2 can be used for noninvasive imaging to determine expression of the therapeutic gene (TK) *in vivo* (11). Second, hSSTR2 can be used for therapy, and the combination of this with TK-mediated prodrug therapy may have an additive or synergistic therapeutic effect. The AdCMVhSSTR2TK was injected intratumorally into A-427 tumors at  $2 \times 10^8$  pfu on days 20 and 27. The <sup>90</sup>Y-SMT 487 was administered intravenously on days 22, 24, 29, and 31 at 18.5 MBq per injection. The GCV was administered intraperitoneally at 50 mg/kg daily for 14 d beginning on day 22. Controls included administration of unlabeled SMT 487 alone, GCV alone, or <sup>90</sup>Y-SMT 487 alone.

Bicistronic Ad vectors encoding for hSSTR2 and the CD enzyme were constructed and tested. Ad vectors expressing CD and hSSTR2 (AdCox-2LCDhSSTR2 and AdCox-2LhSSTR2CD) were produced using the long (L) length Cox-2 promoter. hSSTR2 has been used as a target for noninvasive imaging to determine expression of the therapeutic gene (CD) in vivo (11). Also, hSSTR2 can be used for radioligand therapy, and the combination of this with CD-mediated molecular prodrug therapy may result in radiosensitization. The A-SPECT system ( $\gamma$ -Medica, Inc.) was used for SPECT, with a total of 64 individual projections collected (30 s each) using a 1-mm pinhole collimator. Therapy studies were performed with AdCMVhSSTR2CD injected intratumorally into A-427 tumors at  $1 \times 10^9$  pfu on days 20 and 27.  $^{90}\text{Y}$ -SMT 487 was administered intravenously on days 22, 24, 29, and 31 at 18.5 MBq per injection. The 5-FC was administered intraperitoneally at 400 mg/kg twice a day for 5 d beginning on day 21, followed by another 5-d cycle beginning on day 28.

## Study Results

**Induction of hSSTR2 In Vivo and Localization/Imaging of Radiolabeled Somatostatin Analogs.** Tumor localization of  $^{111}\text{In}$ -DTPA-D-Phe<sup>1</sup>-octreotide in mice bearing intraperitoneal SK-OV-3.ip1 tumors injected intraperitoneally with AdCMVhSSTR2 2 d earlier at 4 h after intraperitoneal injection was 60.4 percentage injected dose per gram (%ID/g), which decreased to 18.6 %ID/g at 24 h after injection (8). Thus, these studies demonstrated that tumor uptake of  $^{111}\text{In}$ -DTPA-D-Phe<sup>1</sup>-octreotide could be achieved after transduction of the ovarian tumor in vivo with AdCMVhSSTR2.

Another study investigated the localization of  $^{111}\text{In}$ -DTPA-D-Phe<sup>1</sup>-octreotide to subcutaneous A-427 non-small cell lung tumors injected intratumorally with AdCMVhSSTR2 (27).  $\gamma$ -Camera imaging showed the tumor uptake of  $^{111}\text{In}$ -DTPA-D-Phe<sup>1</sup>-octreotide to be 2.8 %ID/g at 48 h after injection and 3.1 %ID/g at 96 h. Uptake of  $^{111}\text{In}$ -DTPA-D-Phe<sup>1</sup>-octreotide in control Ad-injected tumors with the thyrotropin-releasing hormone receptor gene (AdCMVTRHr) was  $<0.3$  %ID/g at both time points.

$^{188}\text{Re}$  is a potentially therapeutic radionuclide that can be imaged with a  $\gamma$ -camera.  $^{188}\text{Re}$ -P829 bound with high affinity (6–7 nmol/L) to membrane preparations from A-427 cells infected with AdCMVhSSTR2 (9). Mice bearing subcutaneous A-427 tumors injected intratumorally with AdCMVhSSTR2 showed uptake of intravenously injected  $^{188}\text{Re}$ -P829 detected by  $\gamma$ -camera imaging, whereas uptake was not observed when the tumors were infected with a control Ad. This was confirmed by counting the tumors in a  $\gamma$ -counter, which showed 2.9 %ID/g of  $^{188}\text{Re}$ -P829 in the AdCMVhSSTR2-injected tumors, compared with  $<0.4$  %ID/g in the tumors infected with the control Ad. hSSTR2 expression was independently confirmed by immunohistochemical analysis.

Uptake of  $^{99\text{m}}\text{Tc}$ -P2045 in intraperitoneal SK-OV-3.ip1 tumors in the peritoneum of mice injected intraperitoneally with AdCMVhSSTR2 at 48 h after intravenous injection averaged  $2.2 \pm 0.3$  %ID/g, compared with  $0.2 \pm 0.002$  %ID/g in control mice not receiving Ad injection ( $P < 0.05$ )

or with  $0.3 \pm 0.2$  %ID/g in mice injected intraperitoneally with an Ad encoding the green fluorescent protein (AdCMV-GFP) (28). Images of mice bearing subcutaneous A-427 tumors injected with  $^{99\text{m}}\text{Tc}$ -P2045 showed uptake in the tumors injected with AdCMVhSSTR2 but background uptake in tumors injected with control Ad. The tumor uptake results in the mice 4 d after AdCMVhSSTR2 injection and 4 h after  $^{99\text{m}}\text{Tc}$ -P2045 injection were 7.8 %ID/g. No other tissue had greater uptake than the AdCMVhSSTR2-injected tumor (26). In another study, mice bearing subcutaneous MCF-7 breast tumor xenografts were injected intratumorally with AdCMVhSSTR2GFP. hSSTR2 gene expression was detected with  $^{99\text{m}}\text{Tc}$ -P2045 via  $\gamma$ -camera imaging, and GFP was detected by fluorescent stereomicroscopic imaging (Fig. 1).

**Therapy Studies with the Single-Gene Vector AdCMVhSSTR2.** Untreated animals bearing intraperitoneal SK-OV-3.ip1 tumors had a median survival of 34 d, whereas the median survivals were 36 d after AdCMVhSSTR2 injection and a single 51.8-MBq dose of  $^{64}\text{Cu}$ -TETA-octreotide and 14 d after AdCMVhSSTR2 injection and a single 74-MBq dose. The mice that received 2 doses of  $^{64}\text{Cu}$ -TETA-octreotide (51.8 MBq plus 25.9 MBq) had a median survival of 62 d. Thus, the combination of AdCMVhSSTR2 gene transfer and  $^{64}\text{Cu}$ -TETA-octreotide significantly lengthened survival of the mice. These results establish the key feasibilities of inducing hSSTR2 expression in ovarian tumors and therapy with a radiolabeled somatostatin analog.

Mice bearing subcutaneous A-427 tumors that received 2 intratumoral injections of AdCMVhSSTR2 and four 14.8- or 18.5-MBq doses of  $^{90}\text{Y}$ -SMT 487 had significantly longer median tumor-quadrupling times (40 and 44 d, respectively) than did the mice receiving no treatment and the mice receiving four 18.5-MBq doses of  $^{90}\text{Y}$ -SMT 487 but no virus (16 and 25 d, respectively). The difference in time to tumor quadrupling between the groups that received AdCMVhSSTR2 plus  $^{90}\text{Y}$ -SMT 487 and the control groups was statistically significant.

**Enhancement of Tumor Killing by Radiosensitization Through Molecular Prodrug Therapy.** Subcutaneous A-427 tumors injected with AdCMVhSSTR2 or AdCMVhSSTR2TK

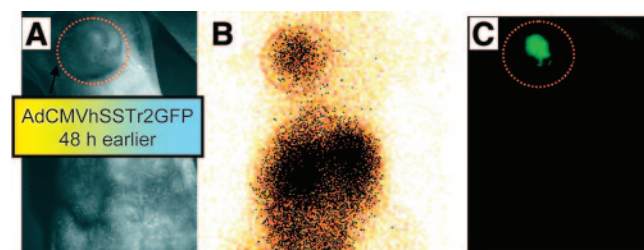


**FIGURE 1.** Dual reporter genes detected by  $\gamma$ -camera imaging and fluorescent imaging. (A) Representative mouse bearing a MCF-7 human breast tumor xenograft was dosed with AdCMVhSSTR2GFP ( $1 \times 10^9$  pfu) and, after 48 h, received intravenous injection of  $^{99\text{m}}\text{Tc}$ -P2045. (B and C) Dual-modality imaging after 5 h included  $\gamma$ -camera imaging (B) and fluorescent stereomicroscopic imaging (C).

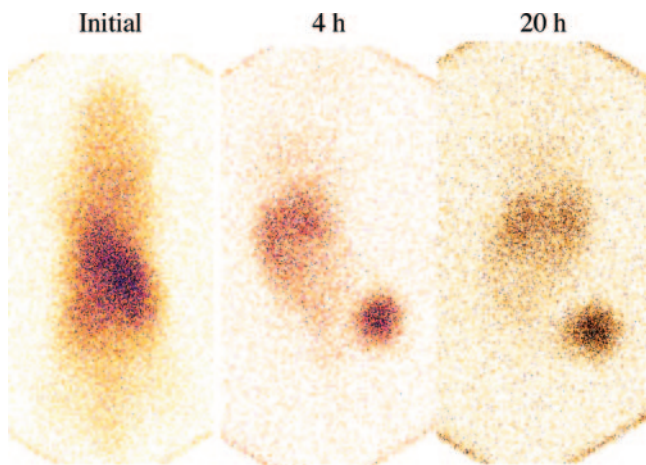


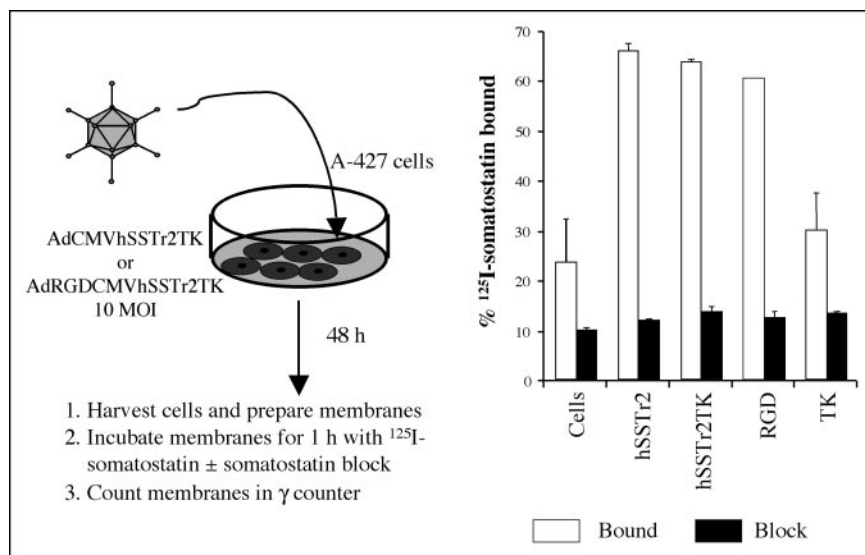
**FIGURE 2.** Imaging of accumulation of  $^{188}\text{Re}$ -P2045 in A-427 tumor previously injected with AdCMVhSSTR2TK.  $^{188}\text{Re}$ -P2045 was injected intravenously 2 d after intratumoral injection of Ad vector. Images were collected initially and after 4 and 20 h.

could be seen by imaging with  $^{99\text{m}}\text{Tc}$ -P2045, and tumors injected with AdCMVhSSTR2TK or AdCMVTK could be seen by imaging with  $^{131}\text{I}$ -FIAU. Tumors injected with AdCMVTK did not accumulate  $^{99\text{m}}\text{Tc}$ -P2045 (11). Uptake of  $^{99\text{m}}\text{Tc}$ -P2045 and  $^{131}\text{I}$ -FIAU for AdCMVhSSTR2TK-injected tumors was 11.1 and 1.6 %ID/g, respectively. AdCMVhSSTR2-injected tumors accumulated 10.2 %ID/g of the  $^{99\text{m}}\text{Tc}$ -P2045 and 0.3% of the  $^{131}\text{I}$ -FIAU. AdCMVTK-injected tumors had 0.2 %ID/g for the  $^{99\text{m}}\text{Tc}$ -P2045 and 3.7 %ID/g for  $^{131}\text{I}$ -FIAU. A separate group of mice bearing a single subcutaneous A-427 tumor (on the right side) was injected intratumorally with AdCMVhSSTR2TK. After 2 d,  $^{188}\text{Re}$ -P2045 was injected intravenously (11.1 MBq) and the mice were imaged. Images from a representative mouse are presented in Figure 2 and demonstrate accumulation of  $^{188}\text{Re}$ -P2045 in the tumor.

Mice bearing intraperitoneal SK-OV-3.ip1 tumors injected with  $1 \times 10^9$  pfu of AdCMVhSSTR2 5 d after tumor

cell inoculation, followed by intraperitoneal injection of  $^{64}\text{Cu}$ -TETA-octreotide 2 d later, had tumor uptake of 25.1 %ID/g at 4 h after  $^{64}\text{Cu}$ -TETA-octreotide administration—a value that was significantly greater than that when the control Ad (AdCMVLacZ) was given (1.6 %ID/g). However, the tumor uptake of  $^{64}\text{Cu}$ -TETA-octreotide after AdCMVhSSTR2 administration decreased to 7.2 %ID/g at 18 h after injection.

*Therapy Studies with the Bicistronic Vector AdCMVhSSTR2TK.* The AdCMVhSSTR2TK bicistronic vector induced a level of hSSTR2 expression in A427 cells equivalent to that induced by the single-gene AdCMVhSSTR2 virus, as shown in Figure 3. Transfected cells were killed after exposure to the prodrug GCV (Fig. 4). Having demonstrated that this bicistronic vector was functionally active, we initiated therapy studies. Table 1 contains the efficacy summary for these studies. The GCV treatment group had the only 2 tumors that regressed. Significant differences were found with respect to tumor-doubling time overall ( $P < 0.001$ ), with multiple comparisons showing that  $^{90}\text{Y}$ -SMT 487 (14.8 MBq  $\times$  4) alone or in combination with GCV had the greatest tumor growth suppression over all treatment groups, with no other significant differences. However, the combination of  $^{90}\text{Y}$ -SMT 487 and GCV resulted in severe toxicity as demonstrated by a dramatic loss of animal weight. Liver toxicity has been reported with Ad-mediated delivery of the TK gene and GCV prodrug administration. The toxicity issue was addressed by reducing the dose of  $^{90}\text{Y}$ -SMT 487 from 18.5 MBq per injection to 14.8 MBq per injection. The results show that tumor inhibition was achieved with  $^{90}\text{Y}$ -SMT 487 alone and with  $^{90}\text{Y}$ -SMT 487 in combination with GCV (Table 1). However, the combination treatment did not improve the results achieved with  $^{90}\text{Y}$ -SMT 487 alone. Toxicity was greatly reduced using 14.8 MBq of  $^{90}\text{Y}$ -SMT 487 instead of the 18.5-MBq dose. In view of the toxicity obtained with the



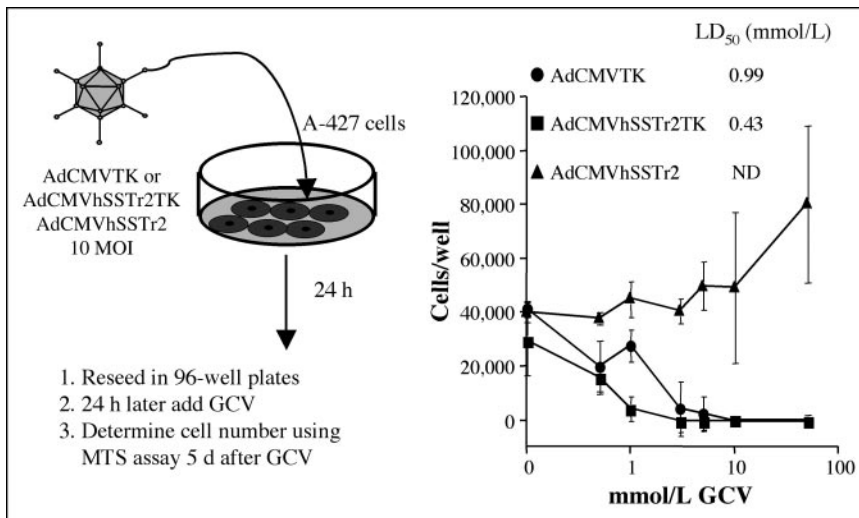


**FIGURE 4.** Evaluation of AdCMVhSSTr2TK bicistronic vectors and AdCMVTK or AdCMVhSSTr2 single-gene vectors for TK activity in infected A-427 cells exposed to GCV.

AdCMVhSSTr2TK vector and radiolabeled peptide, we chose to next investigate the CD/hSSTr2 2 gene vector.

**Therapy Studies with the Bicistronic Vector AdCMVhSSTr2CD.** A-427 cells infected with bicistronic vector AdCMVhSSTr2CD or AdCMVhSSTr2CDRGD, with the RGD peptide genetically engineered in the fiber knob to retarget Ad binding to integrins on the cell surface, had hSSTr2 expression equivalent to that of the single-gene vector AdCMVhSSTr2 (29). In addition, the AdCMVhSSTr2CD and AdCMVhSSTr2CDRGD vectors produced CD enzyme activity levels similar to those of the single-gene vector AdCMVCD (29). Thus, both genes were active in the bicistronic vectors. We next investigated imaging of gene transfer in athymic nude mice bearing subcutaneous A-427 tumors injected with  $1 \times 10^9$  pfu of AdCMVhSSTr2 or AdCMVhSSTr2CDRGD. After 2 d,  $^{99m}\text{Tc}$ -P2045 was intravenously injected and  $\gamma$ -camera imaging demonstrated localization in the tumors (Fig. 5) (30). SPECT was used to measure the distribution of Ad-mediated transgene expression within subcutaneous xenografts. Nude mice bearing 2 A-427 flank tumors were injected intratumorally with AdCMVhSSTr2GFP ( $1 \times 10^9$  pfu) in the right A-427 tumor, and a control bicistronic vector was injected in the left tumor. Imaging studies were conducted after 2 d (Fig.

6). The SPECT technique had sufficient sensitivity and spatial resolution to enable the 3-dimensional hSSTr2 expression to be measured.

Tumor inhibition results in mice with subcutaneous A-427 tumors injected intratumorally with AdCMVhSSTr2 showed that  $^{90}\text{Y}$ -SMT 487 and  $^{90}\text{Y}$ -SMT 487 in combination with 5-FC slowed tumor growth (29). The combination treatment inhibited tumor growth more than did the  $^{90}\text{Y}$ -SMT 487 treatment alone, and the levels of toxicity (weight loss) were modest (29). The next therapy study consisted of radiotargeted gene therapy in combination with external-beam radiation therapy. Tumor inhibition results were encouraging, as they showed that the combination of  $^{90}\text{Y}$ -SMT 487, 5-FC, and  $^{60}\text{Co}$  resulted in tumor regressions (Fig. 7; Table 1). All combination therapies had at least 2 complete regressions, with most being recurrence free. However, the intense triple-therapy regimen was not well tolerated and produced significant weight loss.

**Use of a Tumor-Specific Promoter to Drive Gene Expression.** The specificity of vectors for gene transfer may be improved by combining transductional targeting of Ad using a tumor-specific promoter to drive the transcription of the hSSTr2 and CD genes (30). The liver is the predominant site of Ad vector localization after systemic administration

**TABLE 1**  
Tumor Doubling Times and Complete Regressions in AdCMVhSSTr2TK Experiments

Treatment	n	Tumor doubling time (d)		Complete regressions	
		Mean	Median	Total	No relapse
$^{90}\text{Y}$ -SMT 487 (18.5 MBq $\times$ 4) + GCV	10	8	6	0	0
SMT 487	20	8	7	0	0
GCV (50 mg/kg)	20	14	7	2	2
$^{90}\text{Y}$ -SMT 487 (18.5 MBq $\times$ 4)	10	18	12	0	0
$^{90}\text{Y}$ -SMT 487 (14.8 MBq $\times$ 4) + GCV	10	25	11	0	0
$^{90}\text{Y}$ -SMT 487 (14.8 MBq $\times$ 4)	10	39	38	0	0

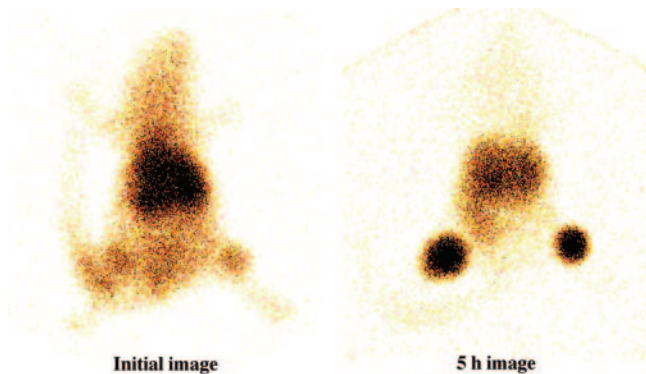


**FIGURE 5.**  $\gamma$ -Camera imaging of gene transfer in mice bearing A-427 subcutaneous tumors injected with AdCMVhSSTR2CD (left) or AdRGDCMVhSSTR2CD (right), followed 2 d later by intravenous injection of  $^{99m}\text{Tc}$ -P2045.

and consequently is at risk when Ad vectors containing suicide genes such as TK or CD localize to this site. Thus, a promoter with both tumor specificity and minimal transcriptional activity in hepatocytes would be ideal for cancer gene therapy. Both AdCox-2LCDhSSTR2 and AdCox-2LhSSTR2CD produced cytotoxicity after infection of DU145 human prostate cancer cells *in vitro* in the presence of 5-FC, with a moderately low value for inhibitory concentration of 50%. Binding of  $^{99m}\text{Tc}$ -P2045 to DU145 cells infected with AdCMVhSSTR2 or AdCox-2LhSSTR2CD was detected in plates by imaging with a  $\gamma$ -camera (30).  $^{99m}\text{Tc}$ -P2045 localization in DU145 subcutaneous tumors injected with AdCox-2LhSSTR2 was demonstrated by  $\gamma$ -camera imaging (30). Another promising approach would be to use a radiation-inducible promoter. Takahashi et al. (31) reported that radionuclides can activate early growth response gene 1 (Egr-1) transcription *in vitro* and arrest the growth of tumor cells transfected with a pEgr-TK plasmid.

**Gene Transfer of the NIS.** Iodide transport into the thyroid gland is mediated by a specific sodium-dependent iodide transporter. This NIS is the plasma membrane glycoprotein responsible for active uptake and concentration of iodide in the thyroid gland, salivary glands, and gastric mucosa (14). The ability of the thyroid gland to accumulate iodide has provided an effective means for imaging and treatment of hyperthyroidism and both primary and metastatic thyroid carcinoma (32).

In 1996, both rat and human NIS complementary DNA was cloned and characterized (33,34). Gene transfer of the NIS gene has been performed with a variety of vectors, cell lines, and tumor xenografts, with successful localization and imaging of tumor xenografts demonstrated after systemic injection of  $^{131}\text{I}$ ,  $^{123}\text{I}$ ,  $^{124}\text{I}$ ,  $^{125}\text{I}$ , and  $^{99m}\text{Tc}$  (13,14,35,36). This approach may also be useful for detection of gene transfer of coexpressed therapeutic genes delivered during gene therapy (15,37). In this regard, Barton et al. (15) imaged CD/TK gene expression in dog prostate using the NIS gene and  $^{99m}\text{Tc}$ .

Therapy studies have been performed on several tumor

xenograft models using this radiotargeted gene therapy approach (14,35,38). The results with  $^{131}\text{I}$  were not always encouraging, because of the rapid cellular efflux of this radionuclide that resulted from a lack of organization in transfected tumors (36,38,39). To deal with this problem, the therapeutic potential of other NIS-transported therapeutic radionuclides with a shorter physical half-life or superior decay properties, including  $^{188}\text{Re}$  and  $^{211}\text{At}$ , has been reported (12,14).

## DISCUSSION

These studies demonstrate that genetic induction of hSSTR2 results in tumor localization of radiolabeled somatostatin analogs at a level sufficient to produce therapeutic effects and that therapeutic efficacy is enhanced by combination with molecular prodrug therapy wherein a second therapeutic gene, TK or CD, is codelivered with the hSSTR2 gene. Efforts continue to optimize this novel approach to cancer gene therapy by the use of radiation-inducible tumor-specific promoters. Another radiotargeted gene therapy approach has been to transfect tumor cells with the noradrenaline transporter to actively accumulate  $^{131}\text{I}$ -metaiodobenzylguanidine (40). This approach has been tested on cells and spheroids but not on animal models. Gene transfer of the NIS has been used successfully for imaging and therapy in preclinical animal models.

The ability to localize radiolabeled ligands or radionuclides within the target tumor provides a new, specific approach to killing cancer cells. The radiotargeted gene

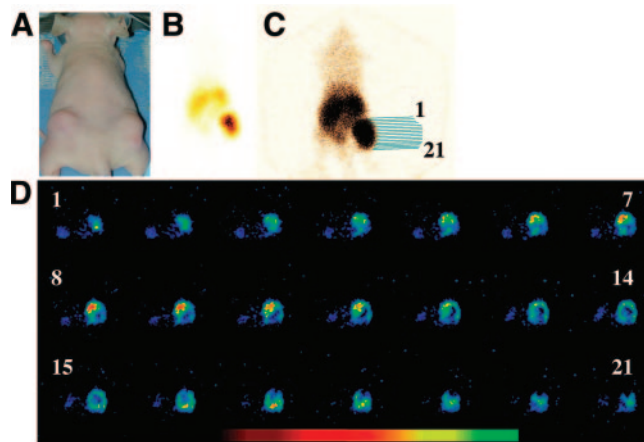


**FIGURE 6.** SPECT of adenovirus-mediated hSSTR2 expression in tumor xenograft. (A) Photograph of representative mouse with 2 A-427 tumors. Right tumor was injected with  $1 \times 10^9$  pfu of AdCMVhSSTR2GFP, and left tumor was injected with control Ad vector. (B and C) Planar  $\gamma$ -camera images obtained 5 h after intravenous  $^{99m}\text{Tc}$ -P2045 injection (55.5 MBq) show that highest retention of  $^{99m}\text{Tc}$ -P2045 was in right tumor. These 2 images are identical, with the exception of scaling. (D) Transverse  $\gamma$ -camera images (0.58-mm slices 1–21 at location shown in C) show hSSTR2 expression within tumor. Adenovirus-mediated hSSTR2 expression led to specific retention of  $^{99m}\text{Tc}$ -P2045 in nonuniform, discrete tumor areas tending to be concentrated at periphery. (Reprinted with permission from (30).)

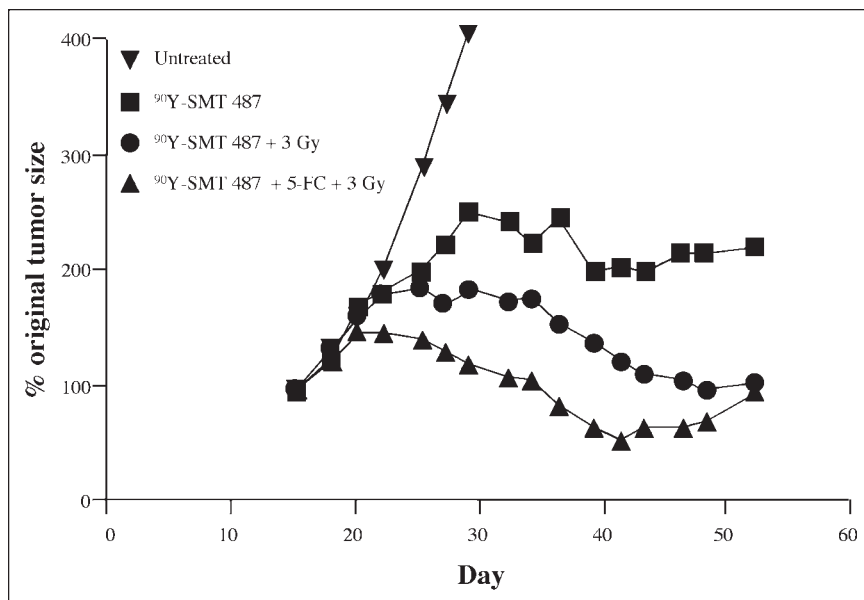


**FIGURE 7.** Therapy results with AdCMVhSSTr2CD, <sup>90</sup>Y-SMT 487, 5-FC, and <sup>60</sup>Co in athymic nude mice bearing subcutaneous A-427 xenografts. AdCMVhSSTr2CD ( $1 \times 10^9$  pfu) was injected into A-427 tumors on days 18, 25, 32, and 39. <sup>90</sup>Y-SMT 487 (18.5 MBq per injection) was administered intravenously on days 20, 22, 27, 29, 34, 36, 41, and 43. 5-FC (400 mg/kg twice a day) was administered intraperitoneally for 5 d beginning on day 19 followed by 3 more 5-d cycles beginning on days 26, 33, and 40. <sup>60</sup>Co external-beam radiation was given as a single 3-Gy dose on days 21, 28, 35, and 42. (Reprinted with permission from (29).)

therapy approach has several advantages. Constitutive expression of a tumor-associated receptor or transporter is not required. Tumor cells are altered to express a new target receptor (hSSTr2) or a transporter (NIS) or to express an existing receptor at higher levels to significantly improve uptake of radiolabeled ligands or radionuclides, compared with uptake in normal tissues. Gene transfer can be effected by intratumoral or regional injection of gene vectors. Another advantage is the feasibility of targeting viral vectors to receptors overexpressed on tumor cells by modifying tropism (binding) or by using tumor-specific promoters such that the virus will specifically be targeted to the desired tumor or the gene product selectively expressed in the tumor. Finally, it is possible to enhance the therapeutic effect by coexpressing the receptor or transporter gene and a second therapeutic gene such as TK or CD for molecular prodrug therapy. However, vector delivery and gene expression are currently limited to locoregional administration.

In conclusion, radiotargeted gene therapy has potential for the treatment of cancer, especially when used in combination with other therapeutic modalities. Clinical studies are needed to determine the most promising of these new therapeutic approaches.

#### ACKNOWLEDGMENTS

Masato Yamamoto, David Curiel, Mark Carpenter, and Buck Rogers are acknowledged for their contributions to the concepts and results presented. The research of the authors is supported in part by Department of Energy grant DE-FG05-93ER61654, Department of Defense grant DAMD17-02-1-0001, and National Institutes of Health contract N01-CO-97110 and grant CA80104.

#### REFERENCES

1. Lamberts SWJ, van der Lely A-J, de Herder WW, et al. Octreotide. *N Engl J Med.* 1996;334:246–254.

- Blum JE, Handmaker H, Rinne NA. The utility of a somatostatin-type receptor binding peptide radiopharmaceutical (P829) in the evaluation of solitary pulmonary nodules. *Chest.* 1999;115:224–232.
- Zamora PO, Gulhke S, Bender H, et al. Experimental radiotherapy of receptor-positive human prostate adenocarcinoma with <sup>188</sup>Re-RC-160, a directly-radiolabeled somatostatin analogue. *Int J Cancer.* 1996;65:214–220.
- Stolz B, Weckbecker G, Smith-Jones PM, et al. The somatostatin receptor-targeted radiotherapeutic [<sup>90</sup>Y-DOTA-DPhe<sup>1</sup>, Tyr<sup>3</sup>]octreotide (<sup>90</sup>Y-SMT 487) eradicates experimental rat pancreatic CA 20948 tumours. *Eur J Nucl Med.* 1998;25:668–674.
- Lewis JS, Lewis MR, Cutler PD, et al. Radiotherapy and dosimetry of <sup>64</sup>Cu-TETA-Tyr<sup>3</sup>-octreotate in a somatostatin receptor-positive, tumor-bearing rat model. *Clin Cancer Res.* 1999;5:3608–3616.
- de Jong M, Krenning E. New advances in peptide receptor radionuclide therapy. *J Nucl Med.* 2002;43:617–620.
- de Jong M, Valkema R, Jamar F, et al. Somatostatin receptor-targeted radionuclide therapy of tumors: preclinical and clinical findings. *Semin Nucl Med.* 2002;32:133–140.
- Rogers BE, McLean SF, Kirkman RL, et al. *In vivo* localization of [<sup>111</sup>In]-DTPA-D-Phe<sup>1</sup>-octreotide to human ovarian tumor xenografts induced to express the somatostatin receptor subtype 2 using an adenoviral vector. *Clin Cancer Res.* 1999;5:383–393.
- Zinn KR, Buchsbaum DJ, Chaudhuri TR, et al. Noninvasive monitoring of gene transfer using a reporter receptor imaged with a high-affinity peptide radiolabeled with <sup>99m</sup>Tc or <sup>188</sup>Re. *J Nucl Med.* 2000;41:887–895.
- Chaudhuri TR, Mountz JM, Rogers BE, et al. Light-based imaging of green fluorescent protein-positive ovarian cancer xenografts during therapy. *Gynecol Oncol.* 2001;82:581–589.
- Zinn KR, Chaudhuri TR, Krasnykh VN, et al. Gamma camera dual imaging with a somatostatin receptor and thymidine kinase after gene transfer with a bicistronic adenovirus. *Radiology.* 2002;223:417–425.
- Carlin S, Mairs RJ, Welsh P, et al. Sodium-iodide symporter (NIS)-mediated accumulation of [<sup>211</sup>At]astatide in NIS-transfected human cancer cells. *Nucl Med Biol.* 2002;29:729–739.
- Chung J-K. Sodium iodide symporter: its role in nuclear medicine. *J Nucl Med.* 2002;43:1188–1200.
- Dadachova E, Carrasco N. The Na<sup>+</sup>/I<sup>-</sup> symporter (NIS): imaging and therapeutic applications. *Semin Nucl Med.* 2004;34:23–31.
- Barton KN, Tyson D, Stricker H, et al. GENIS: gene expression of sodium iodide symporter for noninvasive imaging of gene therapy vectors and quantification of gene expression *in vivo*. *Mol Ther.* 2003;8:508–518.
- Stackhouse MA, Pederson LC, Grizzle WE, et al. Fractionated radiation therapy in combination with adenoviral delivery of the cytosine deaminase gene and 5-fluorocytosine enhances cytotoxic and antitumor effects in human colorectal and cholangiocarcinoma models. *Gene Ther.* 2000;7:1019–1026.
- Woltering EA, O'Dorisio MS, O'Dorisio TM. The role of radiolabeled somatostatin analogs in the management of cancer patients. In: DeVita VT Jr, Hellman

- S, Rosenberg SA, eds. *Principles and Practice of Oncology: PPO Updates*. Vol. 9. 4th ed. Philadelphia, PA: Lippincott-Raven; 1995:1–16.
18. Virgolini I, Leimer M, Handmaker H, et al. Somatostatin receptor subtype specificity and *in vivo* binding of a novel tumor tracer,  $^{99m}\text{Tc}$ -P829. *Cancer Res*. 1998;58:1850–1859.
  19. Manchanda R, Azure M, Lister-James J, et al. Tumor regression in rat pancreatic (AR42J) tumor-bearing mice with Re-188 P2045: a somatostatin analog [abstract]. *Clin Cancer Res*. 1999;5:3769s.
  20. Reubi JC, Schar JC, Waser B, et al. Affinity profiles for human somatostatin receptor subtypes SST1-SST5 of somatostatin radiotracers selected for scintigraphic and radiotherapeutic use. *Eur J Nucl Med*. 2000;27:273–282.
  21. Buscail L, Saint-Laurent N, Chastre E, et al. Loss of sst2 somatostatin receptor gene expression in human pancreatic and colorectal cancer. *Cancer Res*. 1996;56:1823–1827.
  22. de Jong M, Breeman WAP, Bernard BF, et al. [ $^{177}\text{Lu}$ -DOTA $^0$ Tyr $^3$ ] octreotate for somatostatin receptor-targeted radionuclide therapy. *Int J Cancer*. 2001;92:628–633.
  23. Paganelli G, Zoboli S, Cremonesi M, et al. Receptor-mediated radionuclide therapy with  $^{90}\text{Y}$ -DOTA-D-Phe $^1$ -Tyr $^3$ -octreotide: preliminary report in cancer patients. *Cancer Biother Radiopharm*. 1999;14:477–483.
  24. Kwekkeboom DJ, Bakker WH, Kooij PPM, et al. [ $^{177}\text{Lu}$ -DOTA $^0$ Tyr $^3$ ]octreotate: comparison with [ $^{111}\text{In}$ -DTPA $^0$ ]octreotide in patients. *Eur J Nucl Med*. 2001;28:1319–1325.
  25. de Jong M, Kwekkeboom D, Valkema R, et al. Radiolabelled peptides for tumour therapy: current status and future directions—plenary lecture at the EANM 2002. *Eur J Nucl Med Mol Imaging*. 2003;30:463–469.
  26. Rogers BE, Zinn KR, Buchsbaum DJ. Gene transfer strategies for improving radiolabeled peptide imaging and therapy. *Q J Nucl Med*. 2000;44:208–223.
  27. Rogers BE, Zinn KR, Lin C-Y, et al. Targeted radiotherapy with [ $^{90}\text{Y}$ ]-SMT 487 in mice bearing human nonsmall cell lung tumor xenografts induced to express human somatostatin receptor subtype 2 with an adenoviral vector. *Cancer*. 2002;94:1298–1305.
  28. Chaudhuri TR, Rogers BE, Buchsbaum DJ, et al. A noninvasive reporter system to image adenoviral-mediated gene transfer to ovarian cancer xenografts. *Gynecol Oncol*. 2001;83:432–438.
  29. Buchsbaum DJ. Imaging and therapy of tumors induced to express somatostatin receptor by gene transfer using radiolabeled peptides and single chain antibody constructs. *Semin Nucl Med*. 2004;34:32–46.
  30. Buchsbaum DJ, Chaudhuri TR, Yamamoto M, et al. Gene expression imaging with radiolabeled peptides. *Ann Nucl Med*. 2004;18:275–283.
  31. Takahashi T, Namiki Y, Ohno T. Induction of the suicide HSV-TK gene by activation of the Egr-1 promoter with radioisotopes. *Hum Gene Ther*. 1997;8:827–833.
  32. Mazzaferri EL, Kloos RT. Clinical review 128: current approaches to primary therapy for papillary and follicular thyroid cancer. *J Clin Endocrinol Metab*. 2001;86:1447–1463.
  33. Dai G, Levy O, Carrasco N. Cloning and characterization of the thyroid iodide transporter. *Nature*. 1996;379:458–460.
  34. Smanik PA, Liu Q, Furminger TL, et al. Cloning of the human sodium iodide symporter. *Biochem Biophys Res Commun*. 1996;226:339–345.
  35. Cho J-Y, Shen DHY, Yang W, et al. *In vivo* imaging and radioiodine therapy following sodium iodide symporter gene transfer in animal model of intracerebral gliomas. *Gene Ther*. 2002;9:1139–1145.
  36. Dingli D, Peng K-W, Harvey ME, et al. Image-guided radiotherapy for multiple myeloma using a recombinant measles virus expressing the thyroidal sodium iodide symporter. *Blood*. 2004;103:1641–1646.
  37. Niu G, Gaut AW, Ponto LLB, et al. Multimodality noninvasive imaging of gene transfer using the human sodium iodide symporter. *J Nucl Med*. 2004;45:445–449.
  38. Spitzweg C, Dietz AB, O'Connor MK, et al. *In vivo* sodium iodide symporter gene therapy of prostate cancer. *Gene Ther*. 2001;8:1524–1531.
  39. Haberkorn U, Kinscherf R, Kissel M, et al. Enhanced iodide transport after transfer of the human sodium iodide symporter gene is associated with lack of retention and low absorbed dose. *Gene Ther*. 2003;10:774–780.
  40. Boyd M, Mairs RJ, Cunningham SH, et al. A gene therapy/targeted radiotherapy strategy for radiation cell kill by [ $^{131}\text{I}$ ]-meta-iodobenzylguanidine. *J Gene Med*. 2001;3:165–172.

